

Biogeosciences Discussions is the access reviewed discussion forum of *Biogeosciences*

The role of polysaccharides and diatom exudates in the redox cycling of Fe and the photoproduction of hydrogen peroxide in coastal seawaters

S. Steigenberger¹, P. J. Statham², C. Völker¹, and U. Passow¹

¹Alfred Wegener Institut für Polar- und Meeresforschung, Am Handelshafen 12, 27570 Bremerhaven, Germany

²National Oceanography Centre, Southampton, University of Southampton Waterfront Campus, European Way, Southampton SO14 3ZH, UK

Received: 6 March 2009 – Accepted: 17 June 2009 – Published: 30 July 2009

Correspondence to: S. Steigenberger (ss2p07@noc.soton.ac.uk)

Published by Copernicus Publications on behalf of the European Geosciences Union.

Role of polysaccharides and diatom exudates in redox cycling of Fe

S. Steigenberger et al.

Title Page

Abstract

Introduction

Conclusions

References

Tables

Figures

⏪

⏩

◀

▶

Back

Close

Full Screen / Esc

Printer-friendly Version

Interactive Discussion

Abstract

The effect of artificial acidic polysaccharides (PS) and exudates of *Phaeodactylum tricornutum* on the half-life of Fe(II) in seawater was investigated in laboratory experiments. Strong photochemical hydrogen peroxide (H₂O₂) production of 5.2 to 10.9 nM (mg C)⁻¹ h⁻¹ was found in the presence of PS and diatom exudates. Furthermore when illuminated with UV light the presence of algal exudates had a net stabilising effect on ferrous iron in seawater (initial value 100 nmol L⁻¹) above that expected from oxidation kinetics. In the dark the PS gum xanthan showed no stabilising effect on Fe(II). The photochemical formation of superoxide (O₂⁻) in presence of diatom exudates and its reducing effect on Fe(III) appears to result in greater than expected concentrations of Fe(II). A model of the photochemical redox cycle of iron incorporating these processes supported the observed data well. Diatom exudates seem to play an important role for the photochemistry of iron in coastal waters.

1 Introduction

Marine phytoplankton contribute significantly to the CO₂ exchange between atmosphere and ocean, thus impacting on atmospheric CO₂ concentrations (Falkowski et al., 1998). Global marine primary productivity shows great spatial and temporal variability, caused primarily by variable light, zooplankton grazing and nutrient distributions. In addition to the macronutrients (P, N), iron is an essential trace element for photo-autotrophic organisms (Falkowski et al., 1998; Geider et al., 1994; Morel and Price, 2003). Several large scale iron fertilization experiments have revealed that in ~40% of the surface ocean, the so called High Nutrient Low Chlorophyll (HNLC) areas, iron is at least partially responsible for limitation of phytoplankton growth (Boyd et al., 2007). However, iron limitation can occur in coastal areas as well (Hutchins and Bruland, 1998) and here the supply of Fe through upwelling and release from sediments determine its cycling.

BGD

6, 7789–7819, 2009

Role of polysaccharides and diatom exudates in redox cycling of Fe

S. Steigenberger et al.

Title Page

Abstract

Introduction

Conclusions

References

Tables

Figures

⏪

⏩

◀

▶

Back

Close

Full Screen / Esc

Printer-friendly Version

Interactive Discussion

Role of polysaccharides and diatom exudates in redox cycling of Fe

S. Steigenberger et al.

Title Page

Abstract

Introduction

Conclusions

References

Tables

Figures

⏪

⏩

◀

▶

Back

Close

Full Screen / Esc

Printer-friendly Version

Interactive Discussion

Free hydrated Fe(III) concentrations in seawater are very low ($<10^{-20}$ mol L⁻¹, Rue and Bruland, 1995) and the more soluble Fe(II) is rapidly oxidised. (Gonzalez-Davila et al., 2005, 2006; King et al., 1995; Millero and Sotolongo, 1989; Millero et al., 1987). Thus concentrations of dissolved Fe in the ocean should be very low. However, over 99% of the dissolved iron in seawater is reported to be bound by organic compounds (Boye, 2001; Croot and Johansson, 2000; Rue and Bruland, 1995; van den Berg, 1995) and these ligands provide a mechanism whereby the concentrations of dissolved iron typically seen in the ocean can be maintained (Johnson et al., 1997). Iron binding ligands in seawater mainly consist of bacterial siderophores (Butler, 2005; Macrellis et al., 2001) and possibly planktonic exudates like acidic polysaccharides (PS) (Tanaka et al., 1971). Transparent exopolymer particles (TEP), which are rich in acidic polysaccharides, are ubiquitous in the surface ocean (Passow, 2002), and have been shown to bind ²³⁴Th (Passow et al., 2006) and are therefore a prime candidate to also bind iron.

The main oxidation pathway of Fe(II) to Fe(III) is the reaction with O₂ and H₂O₂ according to the Haber-Weiss mechanism (King et al., 1995; Millero and Sotolongo, 1989; Millero et al., 1987). This oxidation can be inhibited (Miles and Brezonik, 1981; Theis and Singer, 1974) or accelerated (Rose and Waite, 2002, 2003a; Sedlak and Hoigne, 1993) in the presence of organic compounds. The decrease in apparent oxidation rate is suggested to be due to stronger photoreduction of Fe(III) in the upper ocean (Kuma et al., 1995) or stabilisation of Fe(II) with organic compounds (Rose and Waite, 2003b; Santana-Casiano et al., 2000, 2004).

In marine systems H₂O₂ functions as a strong oxidant or a reductant (Croot et al., 2005; Millero and Sotolongo, 1989), and thus it is important for the cycling of organic compounds and trace metals including Fe (Millero and Sotolongo, 1989). H₂O₂ is the most stable intermediate in the reduction of O₂ to H₂O and is mainly produced in the water column by photochemical reactions involving dissolved organic matter (DOM) and O₂ (Cooper et al., 1988; Scully et al., 1996; Yocis et al., 2000; Yuan and Shiller, 2001). Light absorbed by DOM induces an electron transfer to molecular oxygen,

forming the superoxide anion radical, which undergoes disproportionation to form hydrogen peroxide. Hence light, O₂, H₂O₂ and organic compounds are important factors in the very complex chemistry of iron in seawater.

Increased photochemical reduction of Fe(III) in the presence of sugar acids has been reported (Kuma et al., 1992; Ozturk et al., 2004; Rijkenberg et al., 2005) but for polysaccharides no such studies have been carried out. However, the relative abundance of polysaccharides in marine dissolved organic matter (DOM) is about 50% (Benner et al., 1992) and in phytoplankton derived DOM the fraction of polysaccharides can be up to 64% (Hellebust, 1965, 1974). In the study reported here we investigate the effect of PS and algal exudates on the photochemical redox cycle of iron and production of H₂O₂.

2 Materials and methods

2.1 General

Three different types of experiments were conducted to investigate the effect of PS and diatom exudates with and without UV light on the speciation of iron and the production of H₂O₂. All experiments were conducted at a constant temperature (about 20°C) in the laboratory. In experiments 1 and 3 samples were exposed to UV radiation using UV transparent 3 L Tedlar bags as incubation containers, whilst in Experiment 2 under dark conditions 30 mL polystyrene screw cap tubes were used.

The natural coastal seawater (SW) used in the experiments was collected in July 2006 off Lepe near Southampton (UK), filtered through 0.2 μm membranes and stored at 5°C in the dark. Organic matter was removed from a portion of this SW via photo-oxidation (see below) with strong UV radiation. The low dissolved organic carbon water, called “organic-free” UVSW (Donat and Bruland, 1988), was also stored at 5°C.

BGD

6, 7789–7819, 2009

Role of polysaccharides and diatom exudates in redox cycling of Fe

S. Steigenberger et al.

Title Page

Abstract

Introduction

Conclusions

References

Tables

Figures

⏪

⏩

◀

▶

Back

Close

Full Screen / Esc

Printer-friendly Version

Interactive Discussion

We used gum xanthan, laminarin and carrageenan (all from Sigma) as the artificial PS. The molecular weight of laminarin is 7700 g mol^{-1} (Rice et al., 2004) and 43% (w/w) of the molecule is carbon. For gum xanthan and carrageenan no specifications could be found but we assumed a carbon content of $\sim 40\%$ (w/w).

5 Diatom exudates were collected as the $0.4 \mu\text{m}$ filtrate of a senescent culture of *Phaeodactylum tricornutum* grown in f/2 medium. Ford and Percival (1965) separated a significant amount of a water-soluble glucan from an aqueous extract of *Phaeodactylum tricornutum*, and their results showed this polysaccharide to be a typical chryso-laminarin with essentially similar properties to the p-1,3-linked glucan, laminarin.

10 Philips 40TL12 and Philips 40T'05 lamps, respectively, were used as a light source for the irradiation of samples with UVB and UVA light during Experiments 1 and 3. Irradiance was measured with a UVA (315–400 nm) sensor type 2.5, a UVB (280–315 nm) sensor type 1.5 (INDIUM-SENSOR, Germany) and a spherical quantum sensor SPQA 2651 (LI-COR) for the photosynthetically active radiation (PAR, 400–15 700 nm). Sensors were coupled to a data logger LI-1400 (LI-COR). The following irradiance values were used for all light incubations during this study: $\text{UVB}=0.3 \text{ W m}^{-2}$, $\text{UVA}=17.6 \text{ W m}^{-2}$ and $\text{PAR}=3.8 \text{ W m}^{-2}$. For all experiments samples were held in UV transparent 3 L polyvinyl fluoride (PVF, Tedlar) bags (SKC Inc., USA), fitted with a polypropylene hose for filling and sub-sampling.

20 2.2 Specific experiments

2.2.1 Experiment 1: Effect of polysaccharides on the photogeneration of H_2O_2

Four pairs of Tedlar bags were filled with MQ water and concentrated solutions of three different PS were added to three pairs of these bags. For this experiment carrageenan, gum xanthan and laminarin were used. The PS were dissolved in MQ water by soni-25 cating for 30 min. The final concentration of PS was 10 mg L^{-1} in about 2.3 L. The last pair of bags served as control and contained no PS. One bag of each pair was placed

[Title Page](#)[Abstract](#)[Introduction](#)[Conclusions](#)[References](#)[Tables](#)[Figures](#)[◀](#)[▶](#)[◀](#)[▶](#)[Back](#)[Close](#)[Full Screen / Esc](#)[Printer-friendly Version](#)[Interactive Discussion](#)

in the dark the other was illuminated with UV light for 270 min. H_2O_2 was measured 1 h before illumination and after 0, 10, 30, 90, 270 min in the light and the dark sample.

2.2.2 Experiment 2: Effect of polysaccharides on the oxidation of Fe(II) in seawater in the dark

5 Ten clean polystyrene screw cap tubes (30 mL) were filled with the natural Solent seawater ($0.2\ \mu\text{m}$ filtered) and another ten tubes were filled with the low organic carbon UVSW. Gum xanthan was added to 5 tubes of SW and 5 tubes of low organic UVSW to give a final concentration of $1\ \text{mg}\ \text{L}^{-1}$ and these samples were sonicated for 30 min. Fe(II) equivalent to $200\ \text{nmol}\ \text{L}^{-1}$ was added to all tubes, and Fe(II) and H_2O_2 measured
10 after 0, 2, 6, 18, and 54 min. Temperature, salinity, oxygen concentration and pH were measured before the iron addition and at the end of the experiment. Sub-sampling was done so that light was excluded.

2.2.3 Experiment 3: Effect of diatom exudates and UVA/B radiation on the oxidation of Fe(II) in seawater

15 Three Tedlar bags were filled with about 1 L of low organic seawater ($0.2\ \mu\text{m}$ filtered). One bag served as a control and no further additions were made. To the second bag $100\ \text{nmol}\ \text{L}^{-1}$ Fe(II) was added. To the third bag additions of diatom exudates and $100\ \text{nmol}\ \text{L}^{-1}$ Fe(II) were made. The amount of diatom exudates added to the sample was chosen in order to reach a concentration of PS similar to that found in natural Solent seawater ($0.4\ \text{mg}\ \text{glucose}\ \text{eq.}\ \text{L}^{-1}$). Ferrous iron concentration was measured
20 over a 60 min period after the iron addition. Samples were UV irradiated for the whole experiment from immediately after the addition of iron to the sample bags. Temperature, salinity, oxygen concentration, pH and total iron were measured before the iron addition and at the end of the experiment. H_2O_2 in the organic-free seawater was ad-
25 justed to an initial concentration of $5\ \text{nmol}\ \text{L}^{-1}$ and was measured again at the end of the experiment.

Role of polysaccharides and diatom exudates in redox cycling of Fe

S. Steigenberger et al.

Title Page

Abstract

Introduction

Conclusions

References

Tables

Figures

⏪

⏩

◀

▶

Back

Close

Full Screen / Esc

Printer-friendly Version

Interactive Discussion

2.3 Analyses

Iron concentrations in the samples were determined using a colorimetric method described by Stookey (1970) and Viollier et al. (2000). Briefly Ferrozine (the disodium salt of 3-(2-pyridyl)-5,6-bis(4-phenylsulfonic acid)-1,2,4-triazine) forms a magenta coloured tris complex with ferrous iron. The water soluble complex is stable and quantitatively formed in a few minutes in the pH range 4–9 after addition of an aqueous 0.01 mol L⁻¹ Ferrozine solution. The absorbance was measured with an Hitachi U-1500 spectrophotometer set at 562 nm in 10 cm cuvettes, with sample pH maintained at 5.5 using an ammonium acetate buffer. Sample concentrations were calculated using a calibration curve made by standard additions to the sample water. Standards were prepared from a 10 mmol L⁻¹ Fe(II) stock solution (Fe(NH₄)₂(SO₄)₂·6H₂O in 0.1 mol L⁻¹ HCl) diluted in 0.01 mol L⁻¹ HCl. Total iron was determined by previous reduction of the iron present in the sample under acid conditions over a 2 h period at room temperature by adding hydroxylamine hydrochloride (1.4 mol L⁻¹ in 5 mol L⁻¹ HCl) as the reducing agent. The detection limit of this method is about 8 nmol L⁻¹ of Fe(II) and the standard error is about 20%. All reagents were from Sigma-Aldrich and at least p.a. grade. All solutions were prepared in MQ water (18 MΩ× cm) purified with a Millipore deionisation system. Samples and standards were prepared in 30 mL polystyrene screw cap tubes. All equipment had been carefully acid washed prior to use.

Concentrations of dissolved mono- and polysaccharides were determined semi quantitatively using the colorimetric method of Myklestad et al. (1997). Briefly the absorbance of the strong coloured complex of 2,4,6-tripyridyl-s-triazine (TPTZ) formed with iron reduced by monosaccharides or previously hydrolyzed polysaccharides at alkaline pH is measured at 595 nm in 2.5 cm cuvettes and compared to a calibration curve prepared from D-glucose in MQ water. Total sugar concentration was determined after hydrolysis of the acidified sample in a sealed glass ampoule at 150°C for 90 min. The detection limit was 0.02 mg glucose eq. L⁻¹ and the standard error was about 3%. All glassware and reagents were prepared as described by Myklestad et al. (1997).

BGD

6, 7789–7819, 2009

Role of polysaccharides and diatom exudates in redox cycling of Fe

S. Steigenberger et al.

Title Page

Abstract

Introduction

Conclusions

References

Tables

Figures

⏪

⏩

◀

▶

Back

Close

Full Screen / Esc

Printer-friendly Version

Interactive Discussion

**Role of
polysaccharides and
diatom exudates in
redox cycling of Fe**S. Steigenberger et al.

Title Page

Abstract

Introduction

Conclusions

References

Tables

Figures

⏪

⏩

◀

▶

Back

Close

Full Screen / Esc

Printer-friendly Version

Interactive Discussion

For the determination of hydrogen peroxide (H_2O_2) a chemiluminescence flow injection analysis (FIA-CL) system as described by Yuan and Shiller (1999) was used. The method is based on oxidation of luminol by hydrogen peroxide in an alkaline solution using Co(II) as a catalyst. Our flow injection system was very similar to that described by Yuan and Shiller (1999) but used a H8443 (Hamamatsu) photo-detector with a power supply and a signal amplifier. The voltage signal was logged every second using an A/D converter and software (PMD-1208LS, Tracer DAQ 1.6.1.0, Measurement Computing Corporation). The chemiluminescence peaks were evaluated by calculating their area. The detection limit was 0.1 nmol L^{-1} and the standard error was 4%. All reagents and solutions were prepared as described by Yuan and Shiller (1999). Since ferrous iron in the sample shows a significant positive interference (Yuan and Shiller, 1999) H_2O_2 was measured in parallel samples without added Fe(II) or after one hour when any initial Fe(II) is expected to be reoxidised.

A WTW 315i T/S system was used to determine temperature and salinity in the sample. Oxygen was measured using a calibrated WPA OX20 oxygen meter. The dissolved organic carbon (DOC) content in the $0.2 \mu\text{m}$ filtered samples was measured with a Shimadzu TOC-VCSN system via high temperature catalytic oxidation (HTCO) on Pt covered Al_2O_3 beads. The detection limit of this method is $\sim 3 \mu\text{mol L}^{-1}$ and the precision is $\pm 2 \mu\text{mol L}^{-1}$.

The UV photooxidation system for the SW consisted of a fan cooled 1 kW medium pressure mercury lamp (Hanovia), with $10 \times 200 \text{ mL}$ quartz tubes mounted around the axial lamp. After 6 h of UV irradiation the samples were considered “organic-free” (UVSW) (Donat and Bruland, 1988). To remove the resulting high concentrations of H_2O_2 the organic-free water was treated with activated charcoal. The charcoal had previously been washed several times with HCl, ethanol and MQ water to remove contaminants. After stirring for 30–40 min the charcoal was removed by filtration through a $0.2 \mu\text{m}$ polycarbonate membrane. The H_2O_2 concentration in the resulting water was less than 0.5 nmol L^{-1} and no contamination with iron was detectable.

2.4 Numerical model

A simple kinetic model to describe the concentrations of Fe(II), Fe(III), O_2^- , and H_2O_2 in experiment 3 was developed on the basis of Weber et al. (2007), similar also to Meunier et al. (2005) or Rose and Waite (2003c). Processes included in the model are listed in Table 1, together with the assumed rate constants for the reactions. Model integrations were done in Matlab, using a variable-order integration method for stiff differential equations. The model contains three parameters that we treat as unknown and that were determined by fitting the model output to the observed concentrations of Fe(II) and H_2O_2 , namely the production rate of superoxide from the interaction of polysaccharides (or more general colored dissolved organic matter) with light, k_{cdom} , the effective photoreduction rate of Fe(III) to Fe(II), k_{red} , and the reduction rate of Fe(III) by superoxide, k_{ro} . As in Meunier et al. (2005) we do not distinguish between different forms (organically complexed or not) of Fe(III), allowing however Fe(III) to be complexed, possibly reducing its effective reaction rate with the superoxide radical (Rose and Waite, 2003c). The fit of the model parameters was done using the Nelder-Meade simplex algorithm, minimizing the root-mean-square (RMS) difference between model and observations, where the deviations were weighted by an estimate of their respective standard error, to make Fe(II)- and H_2O_2 -observations comparable. The Nelder-Meade algorithm is susceptible to ending up in a local minimum of the RMS error; we therefore repeated the optimization several times with different initial guesses for the parameters, to make sure that the global minimum is found.

BGD

6, 7789–7819, 2009

Role of polysaccharides and diatom exudates in redox cycling of Fe

S. Steigenberger et al.

Title Page

Abstract

Introduction

Conclusions

References

Tables

Figures

⏪

⏩

◀

▶

Back

Close

Full Screen / Esc

Printer-friendly Version

Interactive Discussion

3 Results and discussion

3.1 Experiment 1: Effect of polysaccharides on the photochemical production of H₂O₂

The first experiment, examining the effect of polysaccharides on the photochemical production of H₂O₂, showed that within 270 min (4.5 h) of UV illumination large amounts (140–240 nmol L⁻¹) of H₂O₂ were formed due to the presence of 10 mg L⁻¹ of polysaccharides in the MQ water (Fig. 1). The H₂O₂ concentrations in all samples increased linearly during the experiment, when the samples were illuminated. Gum xanthan led to the highest photochemical production of H₂O₂ followed by carrageenan and laminarin, which can be explained by their different absorptivity at <400 nm (Fig. 2). The addition of laminarin led to a net formation rate of H₂O₂ of 22.5 nmol L⁻¹ h⁻¹, which was twice as high as that for pure MQ water (12.3 nmol L⁻¹ h⁻¹). The H₂O₂ formation during illumination of the MQ water was probably due to organic matter leaching from the resin cartridge of the MQ system. However, the DOC concentration in MQ water was <<10 μmol L⁻¹. H₂O₂ formation rates of 36.2 nmol L⁻¹ h⁻¹ and 43.4 nmol L⁻¹ h⁻¹ were measured in samples with added carrageenan and gum xanthan, respectively. The photochemical production of H₂O₂ was thus 3–4 times higher in the presence of carrageenan and gum xanthan compared to pure MQ water. H₂O₂ formation rates of similar magnitude have been reported by Cooper et al. (1988) and Miller et al. (1995) in natural seawater samples. The main structural differences between the molecules of these three PS are that laminarin has a linear structure of linked glucose monosaccharide units, carrageenan has sulphur containing groups and gum xanthan has a branched structure incorporating uronic acid groups. The PS concentration used in our experiment is equivalent to about 4 mg L⁻¹ organic carbon leading to normalised H₂O₂ generation rates of 5.2 nmol L⁻¹ (mg C)⁻¹ h⁻¹ (laminarin), 9.1 nmol L⁻¹ (mg C)⁻¹ h⁻¹ (carrageenan) and 10.9 nmol L⁻¹ (mg C)⁻¹ h⁻¹ (gum xanthan). These values are up to 29 times higher than the rate of 0.38 nmol L⁻¹ (mg C)⁻¹ h⁻¹ reported by Price et al. (1998)

BGD

6, 7789–7819, 2009

Role of polysaccharides and diatom exudates in redox cycling of Fe

S. Steigenberger et al.

Title Page

Abstract

Introduction

Conclusions

References

Tables

Figures

⏪

⏩

◀

▶

Back

Close

Full Screen / Esc

Printer-friendly Version

Interactive Discussion

Role of polysaccharides and diatom exudates in redox cycling of Fe

S. Steigenberger et al.

Title Page

Abstract

Introduction

Conclusions

References

Tables

Figures

⏪

⏩

◀

▶

Back

Close

Full Screen / Esc

Printer-friendly Version

Interactive Discussion

for the >8000 Da fraction of natural DOM in the Western Mediterranean even though the light sources used in our study typically produced only 25% of the UVB radiation 39% of UVA and 1% of PAR of the calculated natural irradiance found in midday summer sun in the Mediterranean (Zepp and Cline, 1977). The polysaccharides in our study caused strong photogeneration of H₂O₂ even under low light exposure probably due to the absence of peroxide destruction processes such as enzymatic decomposition of H₂O₂ (Moffett and Zafiriou, 1990). Reported photochemical production rates of H₂O₂ in the Atlantic Ocean and Antarctic waters are much lower than those reported here, and range from 2.1 to 9.6 nmol L⁻¹ h⁻¹ (Gerringa et al., 2004; Obernosterer, 2000; Yocis et al., 2000; Yuan and Shiller, 2001). Gerringa et al. (2004) calculated a net production rate of 7 nmol L⁻¹ h⁻¹ at irradiance levels of 2.8 (UVB), 43 (UVA) and 346 W m⁻² (VIS/PAR) in 0.2 μm filtered water from the eastern Atlantic close to the Equator. These low rates are presumably due to lower DOC concentrations and higher decay rates due to colloids or enzymatic activity in natural waters (Moffett and Zafiriou, 1990; Petasne and Zika, 1997). Given that H₂O₂ can enhance oxidation of Fe(II), our experiments suggest that PS may have a significant indirect effect on Fe oxidation due to the enhanced photochemical production of H₂O₂.

3.2 Experiment 2: Effect of gum xanthan on the oxidation of Fe(II) in the dark

Changes in the rate of Fe(II) oxidation upon addition of gum xanthan were small, both in the natural SW and the UVSW samples when there was no illumination (Figs. 3 and 4). However, the oxidation of Fe(II) in the natural SW samples (with or without gum xanthan) (Fig. 3) was much slower than that in the respective DOC-free UVSW samples (Fig. 4). Half-life values and oxidation rates of Fe(II) in low-organic seawater by H₂O₂ and oxygen can be calculated according to Millero and Sotolongo (1989) and Millero et al. (1987) respectively. Under our experimental conditions the calculated half-life was 25 s for the ambient H₂O₂ concentrations (270 nM) and 82 s under O₂ saturation. These theoretical values can be compared to measured Fe(II) half-life values of 42 s (UVSW) and 35 s (UVSW+PS). The measured values more closely resemble

the theoretical values under the ambient H_2O_2 conditions. This indicates that the high H_2O_2 concentrations (due to prior removal of organic matter by UV photooxidation) had a stronger oxidising effect on Fe(II) than the dissolved O_2 in the samples.

For the natural SW sample the theoretical half-life of 43 s under O_2 saturation does not fit the measured data well. The half-life of Fe(II) in the natural SW sample (Fig. 3) was ~ 17 times (11.9 min) and with PS added ~ 19 times (13.3 min) longer than the theoretical value. The measured data followed the exponential oxidation curve calculated for the low H_2O_2 concentration (5 nM) of these samples whereas the high O_2 content seemed to not accelerate the measured oxidation of Fe(II).

The DOC content of the natural SW ($97 \mu\text{mol L}^{-1}$) was almost 10 times higher than that in the UVSW. The difference in Fe(II) oxidation between the water types might therefore be due to the stabilisation of Fe(II) against oxidation by natural occurring compounds of the coastal SW (Miles and Brezonik, 1981; Rose and Waite, 2003a; Santana-Casiano et al., 2000, 2004; Theis and Singer, 1974). These results show that the added gum xanthan was not a good model for natural occurring substances stabilising Fe(II) against oxidation. Initial H_2O_2 concentrations also differed appreciably, with $5 \text{ nmol L}^{-1} \text{ H}_2\text{O}_2$ in the natural SW sample and $270 \text{ nmol L}^{-1} \text{ H}_2\text{O}_2$ in the UVSW sample. UV oxidation of the seawater during removal of natural DOC will have led to formation of H_2O_2 . We calculated Fe(II) oxidation rates due to O_2 and H_2O_2 individually in our experiment to investigate if the differing rates could have been caused by differing initial H_2O_2 concentrations. From the comparison between our measured and theoretically calculated values we conclude that a strong effect of H_2O_2 on the lifetime of Fe(II) was observed but no obvious effect of gum xanthan was found in this experiment conducted without irradiation. The lower initial H_2O_2 concentrations in the natural SW sample ($5 \text{ nmol L}^{-1} \text{ H}_2\text{O}_2$; Fig. 3) compared to the UVSW sample ($270 \text{ nmol L}^{-1} \text{ H}_2\text{O}_2$; Fig. 4) appears to be the major cause for slower Fe(II) oxidation, suggesting that H_2O_2 mainly controls the oxidation of Fe(II) in this system.

**Role of
polysaccharides and
diatom exudates in
redox cycling of Fe**S. Steigenberger et al.

[Title Page](#)[Abstract](#)[Introduction](#)[Conclusions](#)[References](#)[Tables](#)[Figures](#)[⏪](#)[⏩](#)[◀](#)[▶](#)[Back](#)[Close](#)[Full Screen / Esc](#)[Printer-friendly Version](#)[Interactive Discussion](#)

3.3 Experiment 3: Effect of diatom exudates and UVA/B radiation on the oxidation of Fe(II) in seawater

Initially, the half-lives of Fe(II) in both treatments, those with and without addition of diatom exudates, was quite similar (Fig. 5). For the initial 5 min (300 s) half lives of Fe(II) in the UVSW without and with added diatom exudates. These values are in the same range as published values (Croot and Laan, 2002; Kuma et al., 1995; Millero et al., 1987). However, a remarkable difference between both treatments is clearly visible after about 420 s (Fig. 5). In the UVSW without exudates the Fe(II) concentration continued decreasing exponentially reaching the detection limit after 20 min, whereas in UVSW with added diatom exudates the Fe(II) concentration remained at about 30 nmol L^{-1} decreasing only very slightly with time. The photochemical effect of the exudates was therefore strong enough to result in a net stabilising effect on Fe(II) after 7 min, confirming results reported by Rijkenberg et al. (2008) who observed irradiance dependent photoreduction of Fe(III) in the presence of the diatom *Thalassiosira sp.*

Differences in H_2O_2 production during the first hour of irradiation were significant between UVSW with and without exudates. In the UVSW sample with added diatom exudates H_2O_2 increased by 33 nmol L^{-1} (from initially 4.6 to 37.6 nmol L^{-1}) over the course of an hour, whereas in pure UVSW the increase was only 5 nmol L^{-1} (from initially 4.3 to 9.7 nmol L^{-1}). This indicates increased photochemical production of H_2O_2 in the presence of exudates. UVSW without exudates contained $11 \mu\text{mol L}^{-1}$ DOC and no measurable total MS and PS, whereas UVSW mixed with exudates of *Phaeodactylum tricornutum* contained $\sim 450 \mu\text{mol L}^{-1}$ DOC, including $0.4 \text{ mg glucose eq. L}^{-1}$ (i.e. $13 \mu\text{mol C L}^{-1}$) total MS and PS. The DOC-normalised H_2O_2 generation of $6.1 \text{ nmol L}^{-1} (\text{mg C})^{-1}$ calculated from 1 h of irradiation of UVSW with exudates indicates that laminarin-like diatom exudates (Ford and Percival, 1965) photochemically produce H_2O_2 . However, the high DOC content suggests that there was also other organic matter contributing to the photo-production of H_2O_2 .

BGD

6, 7789–7819, 2009

Role of polysaccharides and diatom exudates in redox cycling of Fe

S. Steigenberger et al.

Title Page

Abstract

Introduction

Conclusions

References

Tables

Figures

⏪

⏩

◀

▶

Back

Close

Full Screen / Esc

Printer-friendly Version

Interactive Discussion

**Role of
polysaccharides and
diatom exudates in
redox cycling of Fe**S. Steigenberger et al.

[Title Page](#)[Abstract](#)[Introduction](#)[Conclusions](#)[References](#)[Tables](#)[Figures](#)[⏪](#)[⏩](#)[◀](#)[▶](#)[Back](#)[Close](#)[Full Screen / Esc](#)[Printer-friendly Version](#)[Interactive Discussion](#)

Table 1 shows the part of the iron cycle that we think is relevant for our experiment. In pure oxygen containing UVSW the added Fe(II) was oxidised rapidly, but in the presence of diatom exudates either some production of Fe(II) occurred balancing Fe(II) oxidation, or Fe(II) is partly stabilized against oxidation through organic complexation.

As we have found no stabilizing effect of polysaccharides on Fe(II) concentrations in the dark, we assume that the stabilization of Fe(II) is due to a photoreductive process. Photoreduction can occur both directly, presumably as photoreduction of Fe(III) (reaction 1 in Table 1) bound to some organic ligand contained in the exudates, and indirectly via a reaction of Fe(III) with superoxide (reaction 6) that is produced by a light-reaction of dissolved organic matter (reaction 2) (Fujii et al., 2006; Garg et al., 2007a, b; King et al., 1995; Rose and Waite, 2005, 2006; Voelker and Sedlak, 1995; Waite et al., 2006). We used a numerical model based on these assumptions to model the Fe(II) and H₂O₂ concentrations in our experimental system. The initial concentrations for H₂O₂ and Fe(II) in the model were set at 4.6 nmol L⁻¹ and 100 nmol L⁻¹ respectively, all other species were set to zero.

We fitted the model to the observations of Fe(II) and H₂O₂ by varying the production rate of superoxide from the interaction of dissolved organic matter with light, k_{cdom} , the direct photoreduction rate of Fe(III) to Fe(II), k_{red} , and the reduction rate of Fe(III) by superoxide, k_{ro} . Outcomes of the fit are shown in Table 2. Lines 1a and 1b show two different optimal sets of parameters, together with the corresponding minimal value of the RMS difference between model and observations (weighted by the standard deviations in the data). These two different parameter sets belong to two distinct minima of the RMS model data difference that both fit the measurements about equally well (Fig. 6): Both fits reproduce the initial decrease and the subsequent stabilization of the Fe(II) concentration, but not the weak tendency in the latter half of the measurements for a slow decrease in stable Fe(II) concentration. The modelled accumulation of H₂O₂ in the medium is also nonlinear with a rapid initial increase followed by stabilisation near the observed value after one hour.

**Role of
polysaccharides and
diatom exudates in
redox cycling of Fe**S. Steigenberger et al.

[Title Page](#)[Abstract](#)[Introduction](#)[Conclusions](#)[References](#)[Tables](#)[Figures](#)[⏪](#)[⏩](#)[◀](#)[▶](#)[Back](#)[Close](#)[Full Screen / Esc](#)[Printer-friendly Version](#)[Interactive Discussion](#)

Despite the very similar fit to the measurements, the two sets of optimized parameters belong to actually very different descriptions of the redox chemistry in the experiment: The slightly better fit (line 1a in Table 2) has a relatively large direct photoreduction rate of (presumably organically complexed) Fe(III), k_{red} , and a relatively low production rate of superoxide from the interaction of organic matter with light, k_{cdom} . In this model the stabilization of Fe(II) is only achieved by direct photoreduction of Fe(III), not through the superoxide radical. However, this scenario requires an extremely low value of the reduction rate of Fe(III) by superoxide, k_{ro} , on the order of $10^{-6} \text{ M}^{-1} \text{ s}^{-1}$ to reproduce the observed accumulation of H_2O_2 . The reaction rate of superoxide with uncomplexed Fe(III) is $1.5 \times 10^8 \text{ M}^{-1} \text{ s}^{-1}$ (Rose and Waite, 2002), but can be lowered in natural waters by a few orders of magnitude through organic complexation of Fe(III) (Meunier et al., 2005). However, such a low reaction rate is highly improbable in our experimental setup, where Fe(III) concentrations on the order of 80 nM are unlikely to be fully complexed. Although they fit the data slightly less well, we therefore think that the model parameters described in line 1b of Table 2 are a better description of the experiment. In this model fit, the stabilization of Fe(II) is not achieved by direct photoreduction of Fe(III), but through the superoxide radical, which is produced at a rate of $k_{\text{cdom}} = 1.34 \times 10^{-10} \text{ M s}^{-1}$. The estimate of the reaction rate of Fe(III) with superoxide, k_{ro} , is $8.56 \times 10^6 \text{ M}^{-1} \text{ s}^{-1}$, between the values for uncomplexed iron (Rose and Waite, 2002) and those for predominantly complexed iron (Meunier et al., 2005).

To investigate how the estimate of the different rates through our model fit are dependent on each other we performed a set of parameter estimates keeping one of the fitting parameters at a fixed value, and optimizing only the other two. A few messages can be drawn from these additional optimizations that are summarized in lines 2a to 4b in Table 2. Firstly, the optimal parameter values fall into two different classes corresponding to the two results from the unconstrained optimization, with either low values of k_{cdom} and unrealistically low values of k_{ro} , (1a and 3a, maybe 3b), or with high values of k_{cdom} and values of k_{ro} between those found by Rose and Waite (2002) and Meunier et al. (2005) (the rest). Secondly, the model results are also compatible with a higher

direct photoreduction rate k_{red} , such as the value of 10^{-3} s^{-1} observed e.g. by Miller et al. (1995). Thirdly, the values of k_{cdom} in the second class of optimizations (1b, 2a, 2b, 3b, 3c, 4a, 4b and 4c) vary by more than an order of magnitude.

We would conclude from these results that the photochemical formation of Fe(II) is likely to have been dominated by the via light induced (see absorbance spectra Fig. 2) formation of superoxide ($\text{DOM} + h\nu \rightarrow \text{DOM}^*$; $\text{DOM}^* + \text{O}_2^- \rightarrow \text{DOM}^+ + \text{O}_2^-$; and $\text{Fe(III)} + \text{O}_2 \rightarrow \text{Fe(II)} + \text{O}_2^-$) and the subsequent reduction of ferric iron (Fujii et al., 2006; Garg et al., 2007a, b; King et al., 1995; Rose and Waite, 2005, 2006; Voelker and Sedlak, 1995; Waite et al., 2006) with a smaller contribution from direct photoreduction of organically complexed Fe(III). The formation rate of superoxide has probably been in the range between $k_{\text{cdom}} = 10^{-11} \text{ M s}^{-1}$ and $1.5 \times 10^{-10} \text{ M s}^{-1}$ but a more precise determination cannot be made, due to the uncertainty of the rates of direct photoreduction and of the reaction with superoxide and Fe(III) in our setup.

Since the estimated laminarin concentration of $\sim 1 \text{ mg L}^{-1}$ only accounts for $\sim 8\%$ of the DOC content of this sample it is not clear to what extent PS were responsible for the photoreduction during this experiment. Some EDTA (concentration of $\sim 1 \mu\text{mol L}^{-1}$) had inadvertently also been added with the diatom exudates, as it was part of the culture media. However, photoreduction of iron from complexes with EDTA seemed to have had only a minor effect. Reported steady state Fe(II) concentrations due to photoreduction of Fe(III)EDTA complexes (Sunda and Huntsman, 2003) are lower than observed in this study. The reaction quantum yield for the photochemical degradation of Fe(III)EDTA increases strongly with decreasing wavelength ($< 400 \text{ nm}$) (Kari et al., 1995). The UV irradiances (Gehrmann, 1987) of the light source used by Sunda and Huntsman (Vita-Lite, Duro Test) were 1.5 (UVB) to 13.5 (UVA) times lower than in this study. We calculated the concentration of all ferric-EDTA chelate species present in the UVSW sample with exudates added to be 99.7 nmol L^{-1} (MINEQL v3.0) resulting in a steady-state Fe(II) concentration of maximum 8.1 nmol L^{-1} . This accounts only for 27% of the observed 30 nmol L^{-1} which clearly shows a pronounced effect of the added diatom exudates on the steady-state concentration of Fe(II).

Role of polysaccharides and diatom exudates in redox cycling of Fe

S. Steigenberger et al.

Title Page

Abstract

Introduction

Conclusions

References

Tables

Figures

◀

▶

◀

▶

Back

Close

Full Screen / Esc

Printer-friendly Version

Interactive Discussion

Steady state concentrations of photochemical Fe(II) are linearly related to the irradiation energy especially in the UV range (Kuma et al., 1995; Laglera and Van den Berg, 2007; Rijkenberg et al., 2005, 2006). In our study the light intensity was only 25% of the UVB radiation 39% of UVA and 1% of PAR of the calculated natural irradiance in midday summer sun at 40° N (Zepp and Cline, 1977). Therefore under natural coastal conditions, with 4–5 times lower DOC concentrations but a 2.6 to 100 times higher irradiance levels, a photoreductive effect of diatom exudates seems highly probable.

4 Conclusions

In this study we investigated the photochemical effect of artificial and natural polysaccharide material in aquatic systems on iron speciation and on the production of H₂O₂. Artificial PS caused high photochemical production of H₂O₂, which acts as a strong oxidant for metals and organic matter on the one hand, and on the other H₂O₂ is formed photochemically via the superoxide intermediate which is capable of reducing Fe(III). We found increased steady state Fe(II) concentrations in UV illuminated seawater containing a high concentration of exudates of *Phaeodactylum tricornutum*. A stabilisation of Fe(II) in the presence of the artificial PS gum xanthan under dark conditions was not detected. Model results suggest that light-produced superoxide in the presence of exudates of *Phaeodactylum tricornutum* reduces Fe(III), thus maintaining elevated Fe(II) concentrations. In coastal seawater with high content of organic matter originating partly from diatoms an overall positive effect of the exudates on the bioavailability of iron seems likely. Field studies comparing natural ocean waters with and without phytoplankton blooms are needed to confirm these photoreduction results and to examine the counteracting effect of H₂O₂ oxidation over diurnal light cycles, as well as studying these processes as a function of particle size (dissolved, colloidal and particulate fractions).

BGD

6, 7789–7819, 2009

Role of polysaccharides and diatom exudates in redox cycling of Fe

S. Steigenberger et al.

Title Page

Abstract

Introduction

Conclusions

References

Tables

Figures

◀

▶

◀

▶

Back

Close

Full Screen / Esc

Printer-friendly Version

Interactive Discussion

Acknowledgements. We thank P. Goody for his help in the laboratory at the NOCS (UK) and T. Steinhoff and S. Grobe who measured the DOC in our samples at the IfM-Geomar (Germany). Thanks also to N. McArdle for administrative help during this BIOTRACS Early-Stage Training (EST) Fellowship which was funded by the European Union under the 6th Framework Marie Curie Actions. We would also like to thank the CARBOOCEAN project, funded by the European Commission within the 6th Framework Programme, for the financial support of the publication process.

References

- Benner, R., Pakulski, J. D., MacCarthy, M., Hedges, J. I., and Hatcher, P. G.: Bulk chemical characteristics of dissolved organic matter in the ocean, *Science*, 255, 1561–1564, 1992.
- Boyd, P. W., Jickells, T., Law, C. S., et al.: Mesoscale iron enrichment experiments 1993–2005: synthesis and future directions, *Science*, 315, 612–617, 2007.
- Boye, M.: Organic complexation of iron in the Southern Ocean, *Deep-Sea Res. Pt. I*, 48(6), 1477–1497, 2001.
- Butler, A.: Marine Siderophores and Microbial Iron Mobilization, *BioMetals*, 18(4), 369–374, 2005.
- Cooper, W. J., Zika, R. G., Petasne, R. G., and Plane, J. M. C.: Photochemical formation of H_2O_2 in natural waters exposed to sunlight, *Environ. Sci. Technol.*, 22, 1156–1160, 1988.
- Croot, P. L. and Johansson, M.: Determination of iron speciation by cathodic stripping voltammetry in seawater using the competing ligand 2-(2-Thiazolylazo)-p-cresol (TAC), *Electroanalysis*, 12(8), 565–576, 2000.
- Croot, P. L. and Laan, P.: Continuous shipboard determination of Fe(II) in polar waters using flow injection analysis with chemiluminescence detection, *Anal. Chim. Acta*, 466, 261–273, 2002.
- Croot, P. L., Laan, P., Nishioka, J., Strass, V., Cisewski, B., Boye, M., Timmermans, K. R., Klaas R., Bellerby, R. G., Goldson, L., Nightingale, P., and De Baar, H.: Spatial and temporal distribution of Fe(II) and H_2O_2 during EisenEx, an open ocean mesocoscale iron enrichment, *Mar. Chem.*, 95, 65–88, 2005.
- Donat, J. R. and Bruland, K. W.: Direct determination of dissolved Cobalt and Nickel in seawater

BGD

6, 7789–7819, 2009

Role of polysaccharides and diatom exudates in redox cycling of Fe

S. Steigenberger et al.

Title Page

Abstract

Introduction

Conclusions

References

Tables

Figures

◀

▶

◀

▶

Back

Close

Full Screen / Esc

Printer-friendly Version

Interactive Discussion

**Role of
polysaccharides and
diatom exudates in
redox cycling of Fe**S. Steigenberger et al.

[Title Page](#)[Abstract](#)[Introduction](#)[Conclusions](#)[References](#)[Tables](#)[Figures](#)[⏪](#)[⏩](#)[◀](#)[▶](#)[Back](#)[Close](#)[Full Screen / Esc](#)[Printer-friendly Version](#)[Interactive Discussion](#)

by differential pulse cathodic stripping voltammetry preceded by adsorptive collection of cyclohexane-1,2-dione dioxime complexes, *Anal. Chem.*, 60, 240–244, 1988.

Falkowski, P. G., Barber, R. T., and Smetacek, V.: Biogeochemical controls and feedbacks on ocean primary production, *Science*, 281(5374), 200–206, 1998.

5 Ford, C. W. and Percival, E.: The carbohydrates of *Phaeodactylum tricornutum*, *J. Chem. Soc.*, 7035–7041, 1965.

Fujii, M., Rose, A. L., Waite, T. D., and Omura, T.: Superoxide-mediated dissolution of amorphous ferric oxyhydroxide in seawater, *Environ. Sci. Technol.*, 40(3), 880–887, 2006.

Garg, S., Rose, A. L., and Waite, T. D.: Superoxide-mediated reduction of organically complexed iron(III): Impact of pH and competing cations (Ca²⁺), *Geochim. Cosmochim. Ac.*, 71, 5620–5634, 2007a.

Garg, S., Rose, A. L., and Waite, T. D.: Superoxide mediated reduction of organically complexed Iron(III): Comparison of non-dissociative and dissociative reduction pathways, *Environ. Sci. Technol.*, 41(9), 3205–3212, 2007b.

15 Gehrman, W. H.: Ultraviolet Irradiances of Various Lamps Used in Animal Husbandry, *Zoo Biol.*, 6, 117–127, 1987.

Geider, R. J and Roche, J. L.: The role of iron in phytoplankton photosynthesis and the potential for iron-limitation of primary productivity in the sea, *Photosynth. Res.*, 39, 275–301, 1994.

Gerringa, L. J. A., Rijkenberg, M. J. A., Timmermans, K. R., and Buma, A. G. J.: The influence of solar ultraviolet radiation on the photochemical production of H₂O₂ in the equatorial Atlantic Ocean, *J. Sea Res.*, 51, 3–10, 2004.

Gonzalez-Davila, M., Santana-Casiano, J. M., and Millero, F. J.: Oxidation of iron (II) nanomolar with H₂O₂ in seawater, *Geochim. Cosmochim. Ac.*, 69(1), 83–93, 2005.

25 Gonzalez-Davila, M., Santana-Casiano, J. M., and Millero, F. J.: Competition between O₂ and H₂O₂ in the oxidation of Fe(II) in natural waters, *J. Solution Chem.*, 35(1), 95–111, 2006.

Hellebust, J. A.: Excretion of some organic compounds by marine phytoplankton, *Limnol. Oceanogr.*, 10, 192–206, 1965.

Hellebust, J. A.: Extracellular products, in: *Algal physiology and biochemistry*, edited by: Stewart, W. D. P., Blackwell, 838–863, 1974.

30 Hutchins, D. A. and Bruland, K. W.: Iron-limited diatom growth and Si:N uptake ratios in a coastal upwelling regime, *Nature*, 393, 561–564, 1998.

Johnson, K. S., Gordon, R. M., and Coale, K. H.: What controls dissolved iron concentrations in the world ocean? *Mar. Chem.*, 57(3/4), 137, 1997.

- Kari, F. G., Hilger, S., and Canonica, S.: Determination of the Reaction Quantum Yield for the Photochemical Degradation of Fe(III)-EDTA: Implications for the Environmental Fate of EDTA in Surface Waters, *Environ. Sci. Technol.*, 29, 1008–1017, 1995.
- King, D. W., Lounsbury, H. A., and Millero, F. J.: Rates and mechanism of Fe(II) oxidation at nanomolar total iron concentrations, *Environ. Sci. Technol.*, 29, 818–824, 1995.
- Kuma, K., Nakabayashi, S., and Matsunaga, K.: Photoreduction of Fe(III) by hydrocarboxylic acids in seawater, *Water Res.*, 29(6), 1559–1569, 1995.
- Kuma, K., Nakabayashi, S., Suzuki, Y., Kudo, I., and Matsunaga, K.: Photoreduction of Fe(III) by dissolved organic substances and existence of Fe(II) in seawater during spring blooms, *Mar. Chem.*, 37, 15–27, 1992.
- Laglera, L. M. and Van den Berg, C. M. G.: Wavelength dependence of the photochemical reduction of iron in arctic seawater, *Environ. Sci. Technol.*, 41, 2296–2302, 2007.
- Macrellis, H. M., Trick, C. G., Rue, E., Smith, G., and Bruland, K. W.: Collection and detection of natural iron-binding ligands from seawater, *Mar. Chem.*, 76, 175–187, 2001.
- Meunier, L., Laubscher, H., Hug, S. J., and Sulzberger, B.: Effects of size and origin of natural dissolved organic matter compounds on the redox cycling of iron in sunlit surface waters, *Aquat. Sci.*, 67(3), 292–307, 2005.
- Miles, C. J. and Brezonik, P. L.: Oxygen consumption in humic-colored waters by a photochemical ferrous-ferric catalytic cycle, *Environ. Sci. Technol.*, 15(9), 1089–1095, 1981.
- Miller, W. L., King, D. W., Lin, J., and Kester, D. R.: Photochemical redox cycling of iron in coastal seawater, *Mar. Chem.*, 50, 63–77, 1995.
- Millero, F. J. and Sotolongo, S.: The oxidation of Fe(II) with H₂O₂ in seawater, *Geochim. Cosmochim. Ac.*, 53, 1867–1873, 1989.
- Millero, F. J., Sotolongo, S., and Izaguirre, M.: The oxidation kinetics of Fe(II) in seawater, *Geochim. Cosmochim. Ac.*, 51, 793–801, 1987.
- Moffett, J. W. and Zafiriou, O. C.: An investigation of hydrogen peroxide in surface waters of Vineyard Sound with H₂¹⁸O₂ and ¹⁸O₂, *Limnol. Oceanogr.*, 35, 1221–1229, 1990.
- Morel, F. M. M. and Price, N. M.: The biogeochemical cycles of trace metals in the oceans, *Science*, 300, 944–947, 2003.
- Myklestad, S. M., Skanoy, E., and Hestmann, S.: A sensitive and rapid method for analysis of dissolved mono- and polysaccharides in seawater, *Mar. Chem.*, 56(3–4), 279–286, 1997.
- Obernosterer, I. B.: Photochemical transformations of dissolved organic matter and its subsequent utilization by marine bacterioplankton, PhD thesis, 133 pp., 2000.

BGD

6, 7789–7819, 2009

**Role of
polysaccharides and
diatom exudates in
redox cycling of Fe**S. Steigenberger et al.

Title Page

Abstract

Introduction

Conclusions

References

Tables

Figures

◀

▶

◀

▶

Back

Close

Full Screen / Esc

Printer-friendly Version

Interactive Discussion

**Role of
polysaccharides and
diatom exudates in
redox cycling of Fe**S. Steigenberger et al.

[Title Page](#)[Abstract](#)[Introduction](#)[Conclusions](#)[References](#)[Tables](#)[Figures](#)[⏪](#)[⏩](#)[◀](#)[▶](#)[Back](#)[Close](#)[Full Screen / Esc](#)[Printer-friendly Version](#)[Interactive Discussion](#)

- Ozturk, M., Croot, P. L., Bertilsson, S., Abrahamsson, K., Karlson, B., David, R., Fransson, A., and Sakshaug, E.: Iron enrichment and photoreduction of iron under UV and PAR in the presence of hydroxycarboxylic acid: implications for phytoplankton growth in the Southern Ocean, *Deep-Sea Res. Pt. II*, 51, 2841–2856, 2004.
- 5 Passow, U.: Transparent exopolymer particles (TEP) in aquatic environments, *Prog. Oceanogr.*, 55, 287–333, 2002.
- Passow, U., Dunne, J., Murray, J. W., Balistrieri, L., and Alldredge, A. L.: Organic carbon to ²³⁴Th ratios of marine organic matter, *Mar. Chem.*, 100, 323–336, 2006.
- Petasne, R. G. and Zika, R. G.: Hydrogen peroxide lifetimes in south Florida coastal and
10 offshore waters, *Mar. Chem.*, 56, 215–225, 1997.
- Price, D., Mantoura, R. F. C., and Worsfold, P. J.: Shipboard determination of hydrogen peroxide in the western Mediterranean sea using flow injection with chemiluminescence detection, *Anal. Chim. Acta*, 377, 145–155, 1998.
- Rice, P. J., Lockhart, B. E., Barker, L. A., Adams, E. L., Ensley, H. E., and Williams, D. L.:
15 Pharmacokinetics of fungal (1–3)- β -D-glucans following intravenous administration in rats, *Int. Immunopharmacol.*, 4(9), 1209–1215, 2004.
- Rijkenberg, M. J. A., Fischer, A. C., Kroon, J. J., Gerringa, L. J. A., Timmermans, K. R., Wolterbeek, H. T., and De Baar, H. J. W.: The influence of UV irradiation on photoreduction of iron in the Southern Ocean, *Mar. Chem.*, 93, 119–129, 2005.
- 20 Rijkenberg, M. J. A., Gerringa, L. J. A., Carolus, V. E., Velzeboer, I., and de Baar, H. J. W.: Enhancement and inhibition of iron photoreduction by individual ligands in open ocean seawater, *Geochim. Cosmochim. Ac.*, 70(11), 2790–2805, 2006.
- Rijkenberg, M. J. A., Gerringa, L. J. A., Timmermans, K. R., Fischer, A. C., Kroon, K. J., Buma, A. G. J., Wolterbeek, H. T., and De Baar, H. J. W.: Enhancement of the reactive iron pool by
25 marine diatoms, *Mar. Chem.*, 109, 29–44, 2008.
- Rose, A. L. and Waite, T. D.: Kinetic model for Fe(II) oxidation in seawater in the absence and presence of natural organic matter, *Environ. Sci. Technol.*, 36, 433–444, 2002.
- Rose, A. L. and Waite, T. D.: Effect of Dissolved Natural Organic Matter on the Kinetics of Ferrous Iron Oxygenation in Seawater, *Environ. Sci. Technol.*, 37, 4877–4886, 2003a.
- 30 Rose, A. L. and Waite, T. D.: Kinetics of iron complexation by dissolved natural organic matter in coastal waters, *Mar. Chem.*, 84(1–2), 85–103, 2003b.
- Rose, A. L. and Waite, T. D.: Predicting iron speciation in coastal waters from the kinetics of sunlight-mediated iron redox cycling, *Aquat. Sci.-Research Across Boundaries*, 65(4),

375–383, 2003c.

Rose, A. L. and Waite, T. D.: Reduction of organically complexed ferric iron by superoxide in a simulated natural water, *Environ. Sci. Technol.*, 39(8), 2645–2650, 2005.

Rose, A. L. and Waite, T. D.: Role of superoxide in the photochemical reduction of iron in seawater, *Geochim. Cosmochim. Ac.*, 70(15), 3869–3882, 2006.

Rue, E. L. and Bruland, K. W.: Complexation of iron(III) by natural organic ligands in the central North Pacific as determined by a new competitive ligand equilibrium/adsorptive cathodic stripping voltammetric method, *Mar. Chem.*, 50, 117–138, 1995.

Rush, J. D. and Bielski, B. H. J.: Pulse radiolysis studies of the reactions of HO_2/O_2^- with ferric ions and its implications on the occurrence of the Haber-Weiss reaction, *J. Phys. Chem.*, 89, 5062–5066, 1985.

Santana-Casiano, J., Vila, M. G.-D., Rodríguez, M., and Millero, F.: The effect of organic compounds in the oxidation kinetics of Fe(II), *Mar. Chem.*, 70(1–3), 211–222, 2000.

Santana-Casiano, J. M., Gonzalez-Davila, M., and Millero, F. J.: The oxidation of Fe(II) in NaCl- HCO_3^- and seawater solutions in the presence of phthalate and salicylate ions: a kinetic model, *Mar. Chem.*, 85(1–2), 27–40, 2004.

Scully, N. M., McQueen, D. J., Lean, D. R. S., and Cooper, W. J.: Hydrogen peroxide formation: The interaction of ultraviolet radiation and dissolved organic carbon in lake waters along a 43–75 degrees N gradient, *Limnol. Oceanogr.*, 41(3), 540–548, 1996.

Sedlak, D. L. and Hoigne, J.: The role of copper and oxalate in the redox cycling of iron in atmospheric waters, *Atmos. Environ.*, 27A(14), 2173–2185, 1993.

Stookey, L. L.: Ferrozine – a new spectrophotometric reagent for iron, *Anal. Chem.*, 42(7), 779–781, 1970.

Sunda, W. and Huntsman, S.: Effect of pH, light, and temperature on Fe-EDTA chelation and Fe hydrolysis in seawater, *Mar. Chem.*, 84, 35–47, 2003.

Tanaka, Y., Hurlburt, A., Angeloff, L., and Skoryna, S.: Application of Algal Polysaccharides as in vivo Binders of Metal Pollutants, *Proceedings of the International Seaweed Symposium*, 7, 602–604, 1971.

Theis, T. L. and Singer, P. C.: Complexation of Iron(II) by organic matter and its effect on Iron(II) oxygenation, *Environ. Sci. Technol.*, 8, 569–573, 1974.

van den Berg, C. M. G.: Evidence for organic complexation of iron in seawater, *Mar. Chem.*, 50, 139–157, 1995.

Viollier, E., Inglett, P. W., Hunter, K., Roychoudhury, A. N., and Van Cappellen, P.: The ferrozine

BGD

6, 7789–7819, 2009

Role of polysaccharides and diatom exudates in redox cycling of Fe

S. Steigenberger et al.

Title Page

Abstract

Introduction

Conclusions

References

Tables

Figures

◀

▶

◀

▶

Back

Close

Full Screen / Esc

Printer-friendly Version

Interactive Discussion

method revisited: Fe(II)/Fe(III) determination in natural waters, *Appl. Geochem.*, 15(6), 785–790, 2000.

Voelker, B. M. and Sedlak, D. L.: Iron reduction by photoproduced superoxide in seawater, *Mar. Chem.*, 50, 93–102, 1995.

5 Waite, T. D., Rose, A. L., Garg, S., and Fujii, M.: Superoxide-mediated reduction of ferric iron in natural aquatic systems, *Geochim. Cosmochim. Ac.*, Goldschmidt Conference Abstracts, Supplement 1, 70(18), p. A681, 2006.

Weber, L., Völker, C., Oschlies, A., and Burchard, H.: Iron profiles and speciation of the upper water column at the Bermuda Atlantic Time-series Study site: a model based sensitivity study, *Biogeosciences*, 4, 689–706, 2007, <http://www.biogeosciences.net/4/689/2007/>.

10 Yocis, B. H., Kieber, D. J., and Mopper, K.: Photochemical production of hydrogen peroxide in Antarctic Waters, *Deep-Sea Res. Pt. I*, 47(6), 1077–1099, 2000.

Yuan, J. and Shiller, A. M.: Determination of subnanomolar levels of hydrogen peroxide in seawater by reagent-injection chemiluminescence detection, *Anal. Chem.*, 71(10), 1975–1980, 1999.

Yuan, J. and Shiller, A. M.: The distribution of hydrogen peroxide in the southern and central Atlantic ocean, *Deep-Sea Res. Pt. II*, 48, 2947–2970, 2001.

20 Zafiriou, O. C.: Chemistry of the superoxide radical (O_2^-) in seawater, I, pK_{asw}^* (HOO) and uncatalyzed dismutation kinetics studied by pulse radiolysis, *Mar. Chem.*, 31, 31–43, 1990.

Zepp, R. G. and Cline, D. M.: Rates of direct photolysis in aquatic environment, *Environ. Sci. Technol.*, 11(4), 359–366, 1977.

BGD

6, 7789–7819, 2009

Role of polysaccharides and diatom exudates in redox cycling of Fe

S. Steigenberger et al.

Title Page

Abstract

Introduction

Conclusions

References

Tables

Figures

⏪

⏩

◀

▶

Back

Close

Full Screen / Esc

Printer-friendly Version

Interactive Discussion

Role of polysaccharides and diatom exudates in redox cycling of Fe

S. Steigenberger et al.

Table 1. Reactions included in the model and the corresponding kinetic constants. Rates for processes 3, 5 and 7 were calculated for the experimental conditions ($T=22^{\circ}\text{C}$, $S=34.2$, pH 8.1), assuming oxygen saturation.

No.	Reaction	Kinetic parameter	Reference
1	$\text{Fe(III)} + h\nu \rightarrow \text{Fe(II)} + \text{products}$	k_{red}	fitting parameter
2	$\text{CDOM} + \text{O}_2 + h\nu \rightarrow \text{O}_2^- + \text{products}$	k_{cdom}	fitting parameter
3	$\text{Fe(II)} + \text{O}_2 \rightarrow \text{Fe(III)} + \text{O}_2^-$	$1.7 \times 10^{-3} \text{ s}^{-1}$	(Millero et al., 1987)
4	$\text{Fe(II)} + \text{O}_2^- + 2 \text{H}^+ \rightarrow \text{Fe(III)} + \text{H}_2\text{O}_2$	$1.0 \times 10^7 \text{ M}^{-1} \text{ s}^{-1}$	(Rush and Bielski, 1985)
5	$\text{Fe(II)} + \text{H}_2\text{O}_2 \rightarrow \text{Fe(III)} + \text{HO} + \text{HO}^-$	$6.5 \times 10^4 \text{ M}^{-1} \text{ s}^{-1}$	(Millero and Sotolongo, 1989)
6	$\text{Fe(III)} + \text{O}_2^- \rightarrow \text{Fe(II)} + \text{O}_2$	k_{ro}	fitting parameter
7	$2\text{O}_2^- + 2 \text{H}^+ \rightarrow \text{H}_2\text{O}_2$	$3.0 \times 10^4 \text{ M}^{-1} \text{ s}^{-1}$	(Zafiriou, 1990)

Title Page

Abstract

Introduction

Conclusions

References

Tables

Figures

◀

▶

◀

▶

Back

Close

Full Screen / Esc

Printer-friendly Version

Interactive Discussion

Role of polysaccharides and diatom exudates in redox cycling of Fe

S. Steigenberger et al.

Table 2. Best-fit parameters for different optimisation experiments. Parameters that were prescribed rather than optimized are set in brackets.

Optimisation	$k_{\text{red}}[\text{s}^{-1}]$	$k_{\text{cdom}}[\text{M s}^{-1}]$	$k_{\text{ro}}[\text{M s}^{-1}]$	$\log_{10}(\text{RMS})$
1a	1.75×10^{-3}	9.20×10^{-12}	1.47×10^{-6}	1.01
1b	1.33×10^{-5}	1.34×10^{-10}	8.56×10^6	1.12
2a	(0.0)	1.34×10^{-10}	8.57×10^6	1.12
2b	(1.0×10^{-3})	6.22×10^{-11}	3.63×10^6	1.09
3a	1.51×10^{-3}	(0.0)	0.96×10^{-3}	1.18
3b	1.76×10^{-3}	(1.0×10^{-11})	1.93×10^4	1.01
4a	1.74×10^{-3}	1.07×10^{-11}	1.0×10^5	1.01
4b	1.56×10^{-3}	2.40×10^{-11}	1.0×10^6	1.04
4c	6.04×10^{-14}	1.43×10^{-10}	1.0×10^7	1.20

Title Page

Abstract

Introduction

Conclusions

References

Tables

Figures

⏪

⏩

◀

▶

Back

Close

Full Screen / Esc

Printer-friendly Version

Interactive Discussion

**Role of
polysaccharides and
diatom exudates in
redox cycling of Fe**

S. Steigenberger et al.

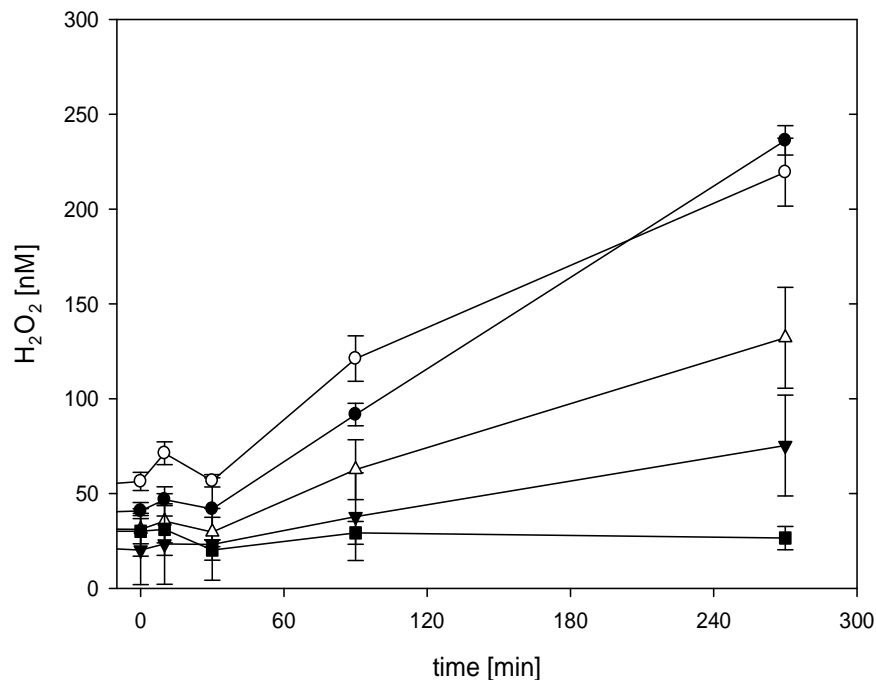


Fig. 1. Photogeneration of H_2O_2 during irradiation of a 10 mg L^{-1} solution of laminarin (open triangle), carrageenan (open circle), gum xanthan (filled circle) and of pure MQ water (filled triangle) and the mean of 4 dark controls (filled squares).

[Title Page](#)[Abstract](#)[Introduction](#)[Conclusions](#)[References](#)[Tables](#)[Figures](#)[◀](#)[▶](#)[◀](#)[▶](#)[Back](#)[Close](#)[Full Screen / Esc](#)[Printer-friendly Version](#)[Interactive Discussion](#)

Role of polysaccharides and diatom exudates in redox cycling of Fe

S. Steigenberger et al.

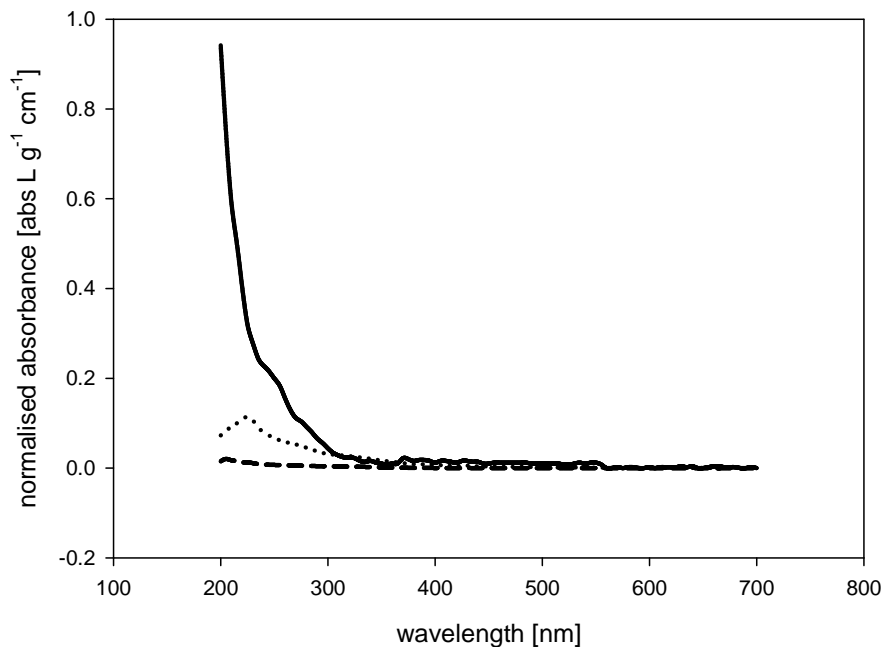


Fig. 2. Absorbance spectra of laminarin (dashed line), carrageenan (dotted line), gum xanthan (solid line) dissolved in MQ water and filtered through 0.2 μm membranes. Absorbances were normalised to 1 g L^{-1} concentration and 1 cm pathlength.

Title Page

Abstract

Introduction

Conclusions

References

Tables

Figures

◀

▶

◀

▶

Back

Close

Full Screen / Esc

Printer-friendly Version

Interactive Discussion

Role of polysaccharides and diatom exudates in redox cycling of Fe

S. Steigenberger et al.

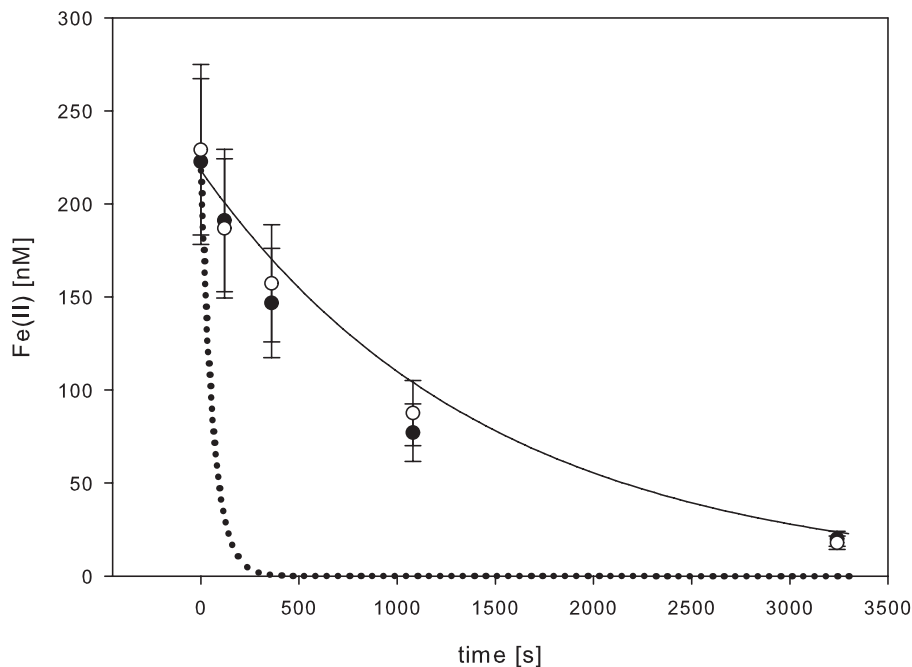


Fig. 3. Dark oxidation of 218 nmol L^{-1} Fe(II) in natural SW (filled circles) and natural SW with PS added. Model results of oxidation of Fe (II) under O_2 saturation (dotted line) and in the presence of 5 nmol L^{-1} H_2O_2 (solid line) at pH 8.4, $S=34.1$, 18°C are also shown.

Title Page

Abstract

Introduction

Conclusions

References

Tables

Figures

◀

▶

◀

▶

Back

Close

Full Screen / Esc

Printer-friendly Version

Interactive Discussion

Role of polysaccharides and diatom exudates in redox cycling of Fe

S. Steigenberger et al.

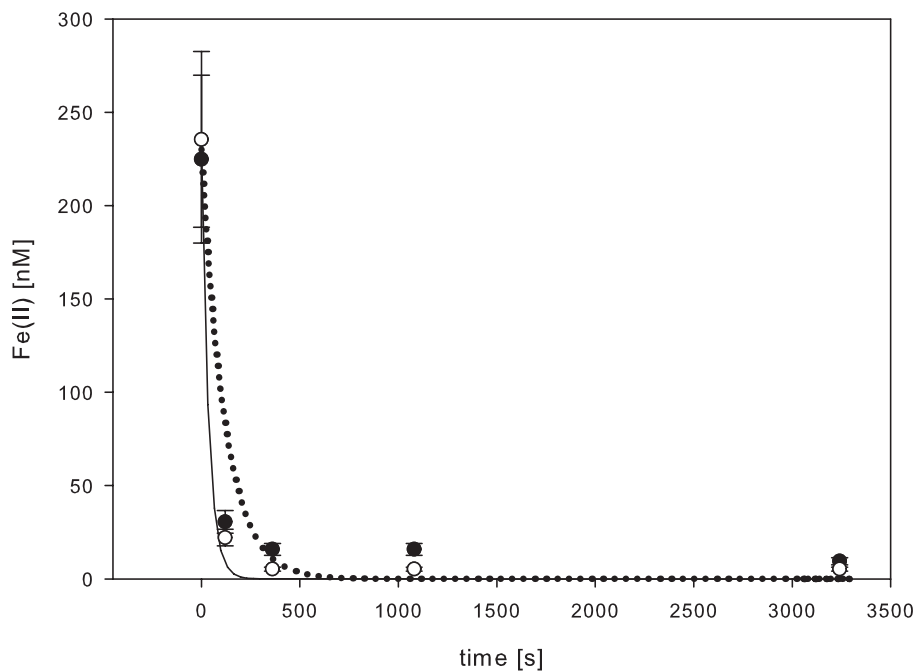


Fig. 4. Dark oxidation of 230 nmol L^{-1} Fe(II) in UVSW (filled circles) and UVSW with PS added. Model results of oxidation of Fe (II) under O_2 saturation (dotted line) and in the presence of 270 nmol L^{-1} H_2O_2 (solid line) at pH 8.3, $S=34.1$, 17°C are also shown.

[Title Page](#)[Abstract](#)[Introduction](#)[Conclusions](#)[References](#)[Tables](#)[Figures](#)[◀](#)[▶](#)[◀](#)[▶](#)[Back](#)[Close](#)[Full Screen / Esc](#)[Printer-friendly Version](#)[Interactive Discussion](#)

Role of polysaccharides and diatom exudates in redox cycling of Fe

S. Steigenberger et al.

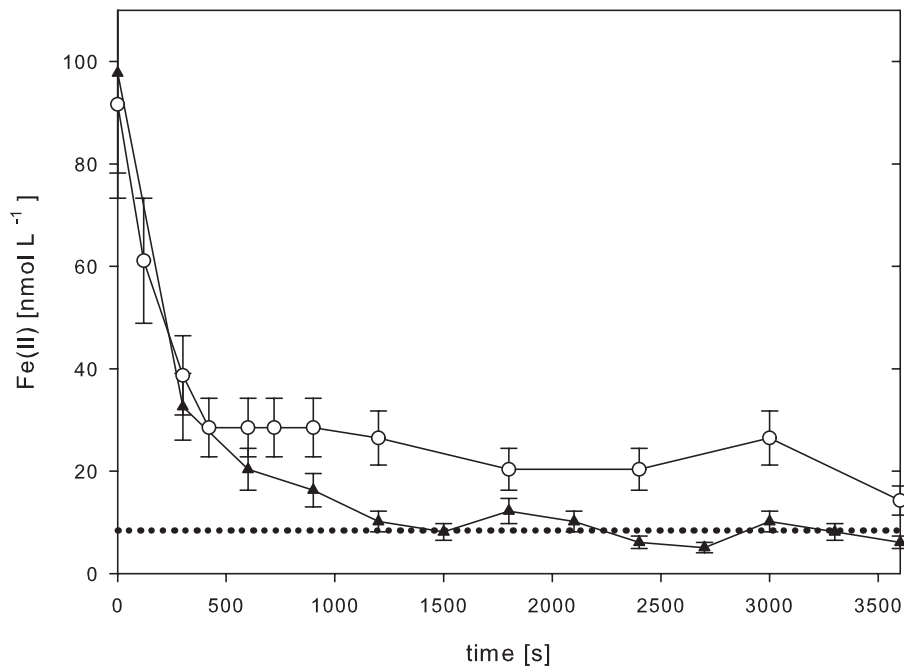


Fig. 5. Oxidation of Fe(II) in pure UVSW (triangles) and in UVSW with added diatom exudates (circles) (22°C , $S=34.2$, O_2 saturated, $\text{pH } 8.1$, $\text{UVB}=0.3\text{ W m}^{-2}$, $\text{UVA}=17.6\text{ W m}^{-2}$, $\text{PAR}=3.8\text{ W m}^{-2}$). The dotted line shows the detection limit.

Title Page

Abstract

Introduction

Conclusions

References

Tables

Figures

◀

▶

◀

▶

Back

Close

Full Screen / Esc

Printer-friendly Version

Interactive Discussion

Role of polysaccharides and diatom exudates in redox cycling of Fe

S. Steigenberger et al.

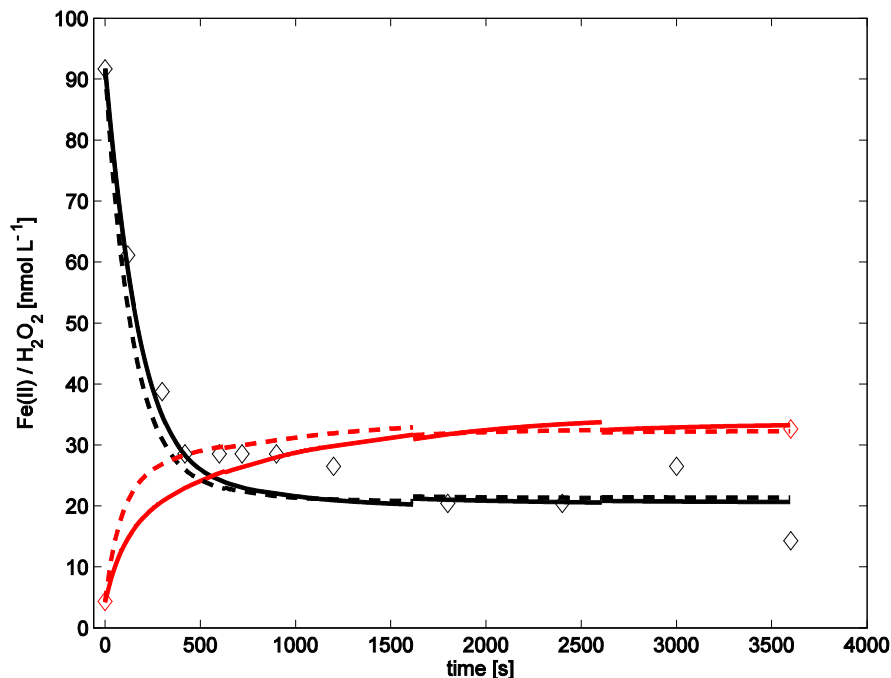


Fig. 6. Best curve fits of the concentration of Fe(II) (black) and H₂O₂ (red) for experimental data of the oxidation of Fe(II) in UVSW with added diatom exudates (Experiment 3: 22°C, pH 8.1, black diamonds show Fe(II), red diamonds show H₂O₂). The dashed lines show respective model fits for Fe(II) and H₂O₂. These two different parameter sets belong to two distinct minima of the RMS (Table 2, lines 1a shown as solid line and 1b shown as dashed line) model data difference that both fit the measurements about equally well: Both fits reproduce the initial decrease and the subsequent stabilization of the Fe(II) concentration, but not the weak tendency in the latter half of the measurements for a slow decrease in stable Fe(II) concentration.

Title Page

Abstract

Introduction

Conclusions

References

Tables

Figures

◀

▶

◀

▶

Back

Close

Full Screen / Esc

Printer-friendly Version

Interactive Discussion